Removal of Thiol Ligands from Surface-Confined Nanoparticles without Particle Growth or Desorption

Edward W. Elliott, III,[†] Richard D. Glover,[†,‡] and James E. Hutchison[*]

Department of Chemistry, University of Oregon, Eugene, Oregon 97403-1253, United States. [†]E.W.E. and R.D.G. contributed equally. [‡]Present address: Bellevue College, Science Division L200, 3000 Landerholm Circle SE, Bellevue, Washington, 98007-6484, United States.

ABSTRACT Size-dependent properties of surface-confined inorganic nanostructures are of interest for applications ranging from sensing to catalysis and energy production. Ligand-stabilized nanoparticles are attractive precursors for producing such nanostructures because the stabilizing ligands may be used to direct assembly of thoroughly characterized nanoparticles on the surface. Upon assembly; however, the ligands block the active surface of the nanoparticle. Methods used to remove these ligands typically result in release of nanoparticles from the surface or cause undesired growth of the nanoparticle core. Here, we demonstrate that mild chemical oxidation (50 ppm of ozone in nitrogen) oxidizes the thiolate headgroups, lowering the ligand's affinity for the gold nanoparticle surface and permitting the removal of the ligands at room temperature by rinsing with water. XPS and TEM measurements, performed using a custom planar analysis platform that permits detailed imaging and chemical analysis, provide insight into the mechanism of ligand removal and show that the particles retain their core size and remain tethered on the surface core during treatment. By varying the ozone exposure time, it is possible to control the amount of ligand removed. Catalytic carbon monoxide oxidation was used as a functional assay to demonstrate ligand removal from the gold surface for nanoparticles assembled on a high surface area support (fumed silica).

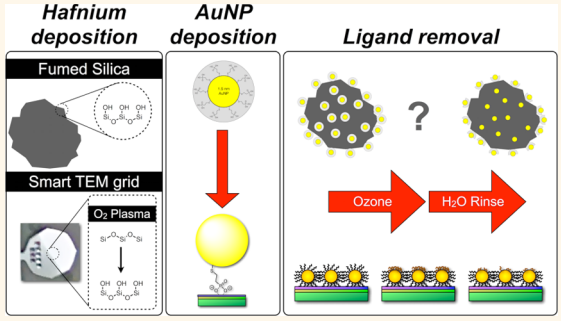

KEYWORDS: gold nanoparticles · self-assembly · ozone · ligand removal · nanoparticle characterization · catalysis

Nanostructures are often used to impart new function to surfaces and hybrid structures with properties tailored to specific applications.[1] These applications take advantage of enhanced functions that derive from size-dependent properties of the nanostructures. For example, gold nanostructures exhibit size-dependent reactivity[2,3] for use in catalytic chemical transformations,[2] semiconductor quantum dot arrays are being harnessed for photovoltaics,[4] and noble metal nanostructures have shown promise for solar to chemical energy conversion.[5,6] In each case, the key catalytic, electronic or optoelectronic properties of the nanostructures are highly sensitive to particle spacing and changes in size. The fabrication of such nanostructures on surfaces with control over both size and surface chemistry remains a major challenge.[2,7−10]

In principle, functionalized, monolayer protected nanoparticles (NPs) can serve as building blocks or precursors to produce well-defined nanostructures on surfaces. Whereas many commonly employed methods to deposit nanostructures (*e.g.*, coprecipitation or deposition-precipitation methods)[3] provide little control over the structure of nanoparticle interfaces or the nanostructure size and uniformity,[11] solution phase synthesis of the nanoparticles affords precise size control and permits detailed characterization. Thus, deposition of preformed nanoparticles onto solid supports permits greater structural control over the nanostructures.[12] Solution-based approaches also allow one to tailor the ligand chemistry to direct self-assembly on the substrate.[13] The nanostructures produced through ligand directed assembly typically retain the size set by the core diameter of the component nanoparticles. However, the stabilizing or directing ligands mask the particle surface, often blocking chemical reactions at the surface or introducing barriers

* Address correspondence to hutch@uoregon.edu.

Received for review December 19, 2014 and accepted February 28, 2015.

Published online March 01, 2015
10.1021/nn5072528

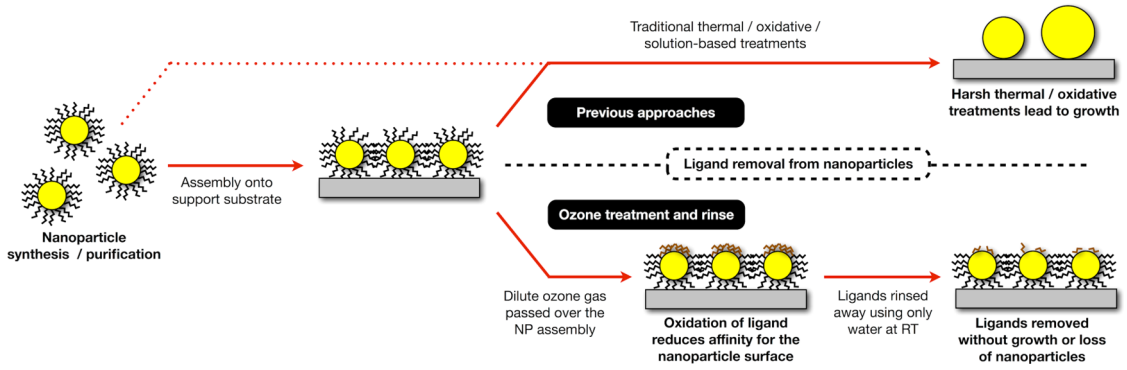

Figure 1. Methods of removing ligands from surface-confined nanoparticles. First, particles of a desired size are synthesized, purified and deposited onto a support substrate. In previous approaches, ligands are typically removed using thermal and oxidative treatments that lead to varying degrees of particle growth and/or loss from the substrate. In contrast, mild chemical treatment using ozone reduces the affinity of the ligands for the particle core affording the room temperature removal of those ligands using water without growth of the core or loss of particles from the support.

to electron transfer. In these cases, the ligands must be replaced or removed.

It is typically challenging to remove the ligand shell without changing the properties of the particles in the assembly. Nanoparticle core growth and loss of material from the support typically occur during ligand removal.[14] A survey of the literature reveals several approaches, often used in concert, for the removal of the ligand shell once a particle is assembled on a surface. These include thermal[11,12] or chemical[15−17] treatments either in the gas phase or in solution (Figure 1).

Early approaches focused on heating the supported nanoparticles in order to vaporize or oxidatively remove the stabilizing ligands.[18,19] These methods are effective for the removal of ligands, but induce varying degrees of particle growth during treatment.[20−25] This growth obviates the advantage in size control when compared with other methods of generating supported gold clusters.

For particles passivated by weakly bound stabilizers, partial removal of the ligand shell and high catalytic activity has been achieved by refluxing supported NPs in water.[12] After 1 h at reflux 20% of the bound carbon was removed. Over the course of 1 and 2 h reflux, the mean NP core diameter increased from 3.0 to 4.8 and 5.7 nm, respectively.[12]

Solvent extraction approaches are not suitable for particles with more strongly bound ligands, such as phosphine or thiols. Alternative approaches involve solution-based oxidation and ligand exchange. Solution-phase oxidation with *t*-butyl hydroperoxide effectively removes triphenylphosphine from gold clusters; however, the clusters underwent morphological changes and particle growth was significant.[15] Another approach to solution-based ligand removal is to displace ligands through the addition of a species with a higher binding affinity for the gold surface (for example, displacing thiol with hydride). Calculations suggest that the binding energies between hydride and a charged gold surface are slightly higher than gold−thiolate bonds. It appears that the exchange of ligands is viable for dispersed nanoparticles, although it does require a large excess of hydride to completely displace the ligand shell.[17] This method has not been demonstrated for surface-confined NPs.

We chose to focus our efforts on the removal of thiol ligands because they are one of the most widely used stabilizers for metal and metal chalcogenide nanoparticles.[26,27] These ligands are popular due to their strong stabilization/passivation of the particle core and the wide variety of terminal functional groups that can be incorporated to control solubility/reactivity and direct the assembly of the particles. To address the challenge of removing the ligand shell while maintaining the NP core size and the NP's attachment to the surface, we investigated whether a mild chemical treatment with ozone could decrease the affinity of thiolate ligands for the surface of the AuNP core and permit ligand removal under mild conditions. Previous work showed that UV/ozone treatment was effective for the removal of self-assembled monolayers (SAMs) from planar gold substrates.[28,29] In these cases, UV irradiation leads to the production of O_3 that oxidizes the organic ligands.[30,31] Previous studies of thiol-stabilized nanoparticles on oxide supports showed that once the ligand shell was oxidized, a subsequent thermal treatment was required to remove the ligand, and this treatment leads to core growth in a manner similar to thermal treatments alone.[16]

Herein, we report a mild chemical oxidation that lowers the affinity of thiol ligands for the surface of gold nanoparticles, facilitating ligand removal with water rinsing at room temperature. Under these conditions, the NPs remain firmly bound to the substrate and core size remains the same. The extent of ligand removal can be controlled by varying the duration of oxidation. Carbon monoxide oxidation, used as a functional assay, confirms that a catalytically active gold surface results from ligand removal.

RESULTS AND DISCUSSION

A strategy was needed to analyze the function, composition and structure of the AuNPs on a substrate after assembly and ligand removal. It is relatively easy to assess the functional activity of the NPs on the high surface area supports typically used in catalytic, sensing and electrochemical applications owing to the relatively large surface area that can be exposed on a three-dimensional sample. It is more difficult to assess core size and size variation of statistically representative populations on these supports because the support often obscures direct imaging of the nanoparticles and/or makes it difficult to focus on all the NPs simultaneously. For these reasons, it is even more challenging to assess transformations in size as a result of thermal or chemical treatments. In addition, the surface chemistry of the NPs on three-dimensional substrates is difficult to analyze because these signals are obscured by strong signals from the substrate and there is significant sample-to-sample variation in surface roughness.[32] For monitoring size changes, nanoparticle loss and chemical transformations, monolayer assemblies on a planar substrate are much more appropriate. However, it is not typically feasible to assess the functional (catalytic) properties of NPs on such a planar platform because there is so little active surface area (~ three million times less than on 100 mg of fumed silica). Consequently, a we developed a tandem strategy wherein the same NP surface chemistry can be employed on (i) a surface permitting detailed structural and surface analysis[33] and (ii) a high surface area substrate suited for functional assessment.[34]

Ligand-stabilized AuNPs were assembled on two types of silicon dioxide substrates to permit structural, chemical and functional analysis of the products following ozone treatment. Microscale fumed silica particles offer a high surface area support (200 m^2/g) that can bind a sufficient number of nanoparticles making it possible to evaluate the function of the nanoparticles by assessing the catalytic activity of the nanoparticles toward CO oxidation.[35] A second substrate, a planar analysis platform (Smart Grid), permits detailed structural and surface analysis, by transmission electron microscopy (TEM) and X-ray photoelectron spectroscopy (XPS), respectively.

The same surface attachment chemistry can be used to assemble the NPs on the surface in both cases. Terminal phosphonate groups on the periphery of thiol-stabilized gold nanoparticles direct the assembly of the particles onto a Hf(IV)-treated silicon dioxide surface (Figure 2). The hafnium binds to the free silanol groups on the SiO_2 surface and subsequently binds the phosphonate groups, resulting in immobilization of the nanoparticles on the surface.[36,37]

Synthesis and Assembly of 1.4 nm 2-MEPA AuNPs. AuNPs synthesized for this study possess phosphonate-terminated thiol ligands that direct assembly of the NPs on silica surfaces and small core sizes active toward CO reduction.[34,38] Synthesizing the AuNPs in solution, independent of the support, allowed for control over size. Because the ligands are strongly bound, it is possible to rigorously purify the NPs to remove extraneous species (which can complicate subsequent assembly steps) following synthesis.[3,39] The AuNPs (d_{core} = 1.4 ± 0.4 nm) functionalized with (2-mercaptoethyl)phosphonic acid (2-MEPA) were synthesized using a previously described method and utilized for all experiments in this study.[38] Nanoparticles were purified by diafiltration to ensure that free ligand and extraneous ions from the gold salt were completely removed. Purification is important as the presence of free ligand would impede self-assembly[39] and the presence of halides during ligand removal has previously been shown to encourage growth of the gold clusters during ligand removal.[40,41]

Assembly of the 1.4 nm 2-MEPA AuNPs on Hf(IV) treated silica substrates followed the approach previously reported in the literature.[33,34,36] Fumed silica microparticles were soaked in 5 mM $HfOCl_2$ to functionalize the silanol-rich SiO_2 surface and then rinsed with nanopure water. To assemble the nanoparticles, the Hf-treated silica was immersed in a 3:1 methanol/water solution containing 1.6 mg of AuNPs per mL of solution. After completion of the assembly process, the derivatized silica was purified by several rounds of centrifugation and resuspension in nanopure water. The AuNP loading was confirmed by ICP-OES following digestion of the sample in *aqua regia*. Results from this experiment indicated a final gold loading of 2.1 wt %. This relatively high loading of discrete AuNPs is appropriate for functional assays involving CO oxidation.

TEM micrographs of the samples before and after nanoparticle assembly (Figure 3) confirmed the presence of small NPs on the surface of the support, but did not permit rigorous quantification of nanoparticle size due to the small core diameters, overlap of neighboring particles and the limited depth of field. Qualitative analysis of nanoparticles that are in the same focal plane yields an average size of ~2 nm. The three-dimensional nature of these samples makes it difficult to perform more quantitative measurements of core changes and to investigate changes in the surface chemistry.

A planar analysis platform (Smart Grid) was designed and used to fully characterize the changes in surface chemistry and NP morphology of the assemblies by XPS and TEM. Photolithography was used to etch an octagonal analysis platform from silicon (Figure 4). One half of the 3 mm diameter platform is a grid of thermally grown, electron transparent SiO_2 windows suitable for direct TEM imaging of the NP assemblies. The other half is a smooth surface with more underlying material to prevent charging, making it more suitable for XPS analysis. The entire surface of the platform is thermally grown silicon dioxide.

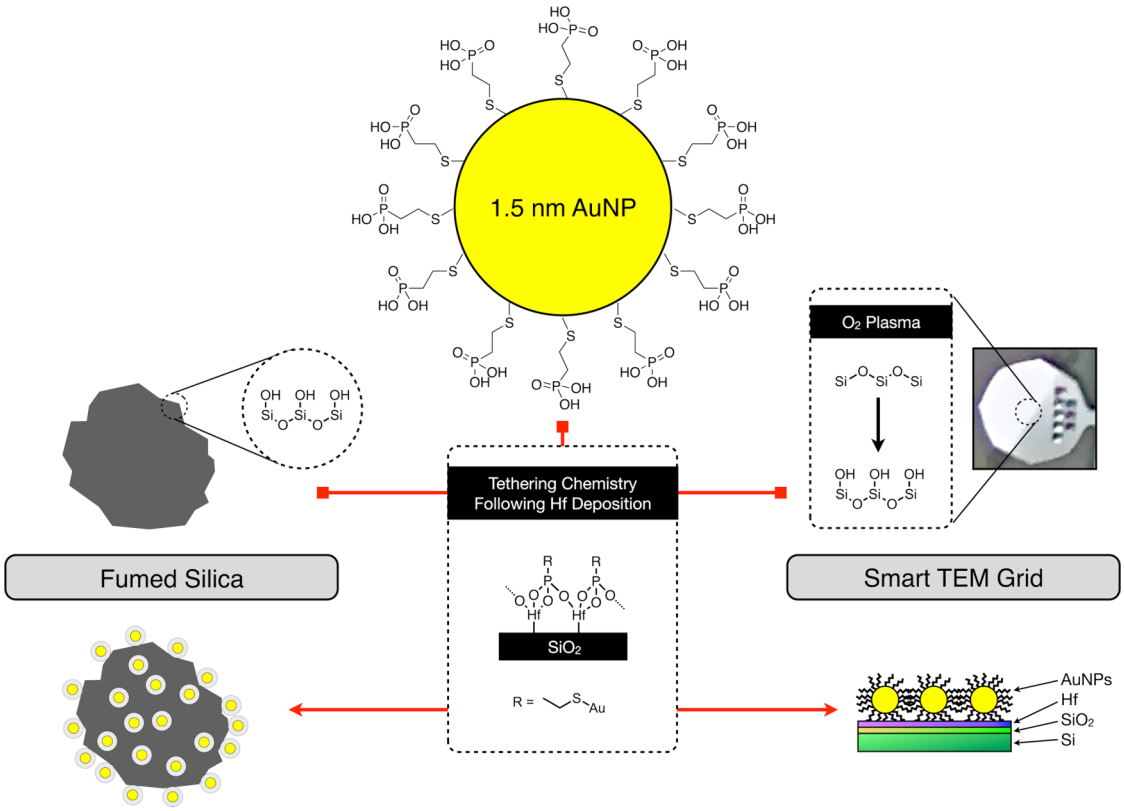

Figure 2. Assembly of 2-MEPA functionalized AuNPs onto both a high surface area support (fumed silica) and a planar analysis platform based on Smart Grid TEM grids. In either case the tethering chemistry is the same: Hf(IV) binds to surface silanols on the support and serves to anchor the AuNPs to the surface through the NP's terminal phosphonate groups.

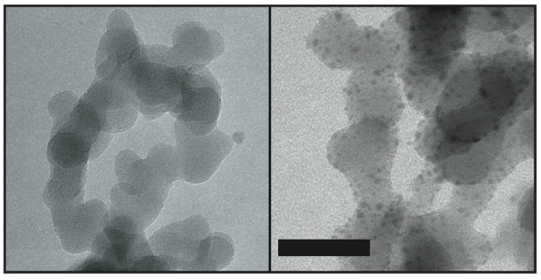

Figure 3. TEM micrographs of fumed silica before (left) and after (right) assembly of 1.4 nm 2-MEPA AuNPs. Scale bar shown is 50 nm. Assembly was accomplished by soaking fumed silica in a 5 mM $HfOCl_2$ solution and then utilizing the terminal phosphonate on the stabilizing thiol ligand (2-MEPA) to bind the nanoparticles.

The chemical treatment used to assemble NPs on the Smart Grid was the same as for the fumed silica support. To ensure that the Smart Grid has a high density of surface hydroxyl groups, comparable to that found on fumed silica, grids were first treated with O_2 plasma prior to the Hf(IV) soak.[42] Removal of weakly bound NPs or other impurities was done by simply rinsing the grid with nanopure water.

XPS was used to determine the chemical composition of the NPs on the surface. In particular, the oxidation state of the sulfur can be determined. Surface roughness and differences in attenuation lengths can complicate analysis of nanostructures by XPS. To circumvent these limitations, we used the planar analysis platform (etched from a silicon wafer), assembled a single monolayer of nanoparticles, and confirmed that core sizes were maintained throughout the analysis. By so doing, we avoided differences in surface roughness and signal attenuation that might normally make it difficult to compare spectra for nanostructured samples.

In the assembled samples, XPS analysis confirms that the sulfur is in the thiolate form (Figure 4). TEM micrographs of the AuNPs on the planar platform following assembly showed that coverage was similar to the high surface area supports and further analysis determined the diameter of the AuNPs following deposition to still be 1.4 ± 0.4 nm (Figure 4).[43]

Removal of Ligands from Supported AuNPs Using a Dilute Ozone Treatment. In order to unmask the gold surfaces of the AuNPs without NP desorption or core size changes, we investigated the oxidation of thiol ligands by O_3. Initial experiments with UV/O_3 generators produced large (15−20 nm diameter), often nonspherical NPs. It also proved difficult to control and quantify ozone exposure. To address these issues, AuNP assemblies were treated with O_3 generated *ex situ* by a corona generator supplied with dry air. This concentration of ozone (~500 ppm) led to oxidation and significant growth of the AuNPs within the first few minutes (Figure S1, Supporting Information). Thus, the O_3 was diluted with nitrogen using air flow meters to produce a

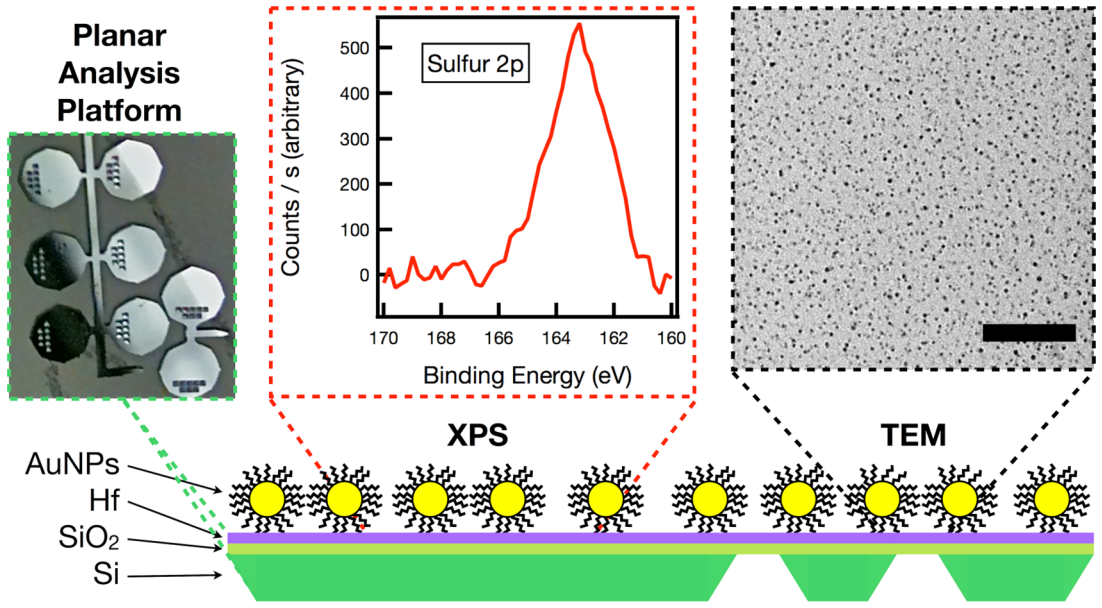

Figure 4. Schematic of the analysis strategy used to evaluate ozone-mediated oxidative ligand removal on the planar assembly. 1.4 nm AuNPs were attached to custom Smart Grids with only half of the surface containing windows, shown left. The portion of the substrate without windows reduces charging and facilitates XPS analysis (center). The portion with windows affords the direct observation of AuNPs by TEM (right, scale bar = 50 nm). The combination of techniques permits detection of subtle morphological and chemical changes between treatment steps.

final O_3 concentration of 50 ppm. Under these conditions it is possible to slow the oxidation and precisely control the exposure of the ligand shell. Both the planar and high surface-area assemblies were treated with dilute ozone as described in the Methods section.

XPS analysis of ozone-treated 1.4 nm 2-MEPA AuNPs on the planar analysis platform showed changes in the amount and oxidation state of sulfur in the ligand shell over the course of treatment. The S 2p peaks were initially difficult to quantify using curve fitting algorithms due to interference from the underlying silicon plasmon loss feature. To address this we performed background subtraction from a sample without gold nanoparticles resulting in flatter baselines. Following baseline correction the peak area, representing relative amounts of bound reduced-sulfur (B.E. = 162 eV) and oxidized sulfur (B.E. = 168 eV) were determined.[44−46] Changes to the type of sulfur species present before treatment, after 8 min of exposure to 50 ppm ozone, and finally after the subsequent water rinse are shown in Figure 5.

XPS data are consistent with a portion of the ligand shell being oxidized, as evidenced by the presence of both bound thiolate and oxidized sulfur species following exposure to dilute ozone. Previous literature indicated that the oxidized sulfur may be strongly associated with the gold surface;[16] however, the reduction in the signals due to oxidized sulfur suggest the majority of the oxidized species are easily removed at room temperature by water rinsing. Observation of the residual bound thiolate suggests that some of the ligand shell is resistant to oxidation, providing a stable tether between the AuNPs and the support.

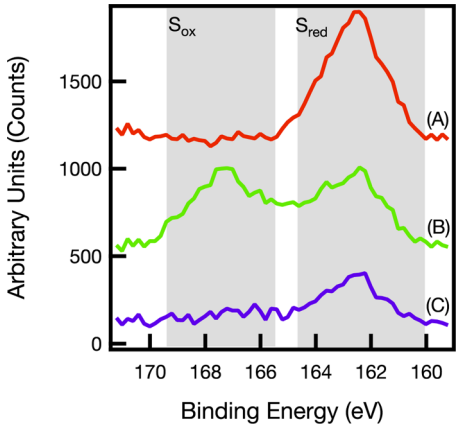

Figure 5. Stacked plot of XPS spectra for S 2p illustrating the influence of ligand oxidation and removal. Red trace (A) represents AuNPs as assembled on the planar substrate. Green trace (B) represents nanoparticles after 8 min of dilute ozone treatment. Purple trace (C) represents the ozone-treated sample following an 11 min nanopure water rinse. Contributions from sulfur bound to gold appear near 162 eV (S_{red}), whereas oxidized sulfur species have a binding energy near 168 eV (S_{ox}).

Quantifying Nanoparticle Stability Over the Course of Ligand Removal. Following ozone treatment and removal of oxidized ligand by soaking in water, TEM analysis of the planar substrate suggested no significant nanoparticle loss (Figure S2). To corroborate these data, we quantified by ICP-OES the amount of gold that was lost following the oxidation of gold particles attached to fumed silica. Because of the higher surface area and increased hindrance to accessing the surface compared to the planar system, the ozone treatment time was increased to 20 min. Following ozone treatment

TABLE 1. AuNP Core Diameter Following Ligand Removal with Ozone Treatment and Water Rinsing

ozone treatment (min)	size following treatment and rinse[a] (nm)	number of particles analyzed
no treatment	1.4 ± 0.4	5392
4	1.4 ± 0.3	6759
8	1.4 ± 0.4	3564
16	1.6 ± 0.6	3273

[a] Gold nanoparticle diameter and polydispersity were determined by TEM analysis on the Smart Grid (Figure S2) during ozone treatment between 4 and 16 min, followed by an 11 min soak in nanopure water to remove oxidized ligand.

the high surface area support assembly was soaked in nanopure water for 11 min and the supernatant was collected and analyzed by ICP-OES. The recovered supernatant indicated a negligible loss of gold (<0.2 wt % of gold loaded on the fumed silica support). These data demonstrate that particles are not lost from the surface. Taken together with the fact that some of the gold thiolate bonds are not oxidized during treatment, this suggests that these remaining covalent linkers continue to tether the AuNPs to the substrate.

TEM measurements were also used to determine whether nanoparticle growth occurs when ligands are no longer present to prevent coalescence of neighboring AuNPs. AuNPs on the planar assemblies were exposed to the dilute ozone stream for up to 16 min. These samples were then soaked for 11 min in 20 mL of nanopure water, dried under a stream of argon, and finally analyzed by TEM (Table 1). For ozone treatment times up to 8 min, the core sizes remained constant even after the removal of oxidized ligand. Only after the planar system was exposed to dilute ozone for twice that time did the TEM images of the particles show evidence of slight growth following the water soak (from 1.4 ± 0.4 to 1.6 ± 0.6 nm).

Ligand Removal Produces Catalytically Active Gold Sites. To examine whether ligand removal produces a catalytically active gold surface following ozone treatment and rinsing, the oxidation of CO was evaluated for NPs on the high surface area (fumed silica) support. The room temperature oxidation of CO was chosen, because the reaction is sensitive to both the preparation method of the supported AuNPs as well as the final gold cluster size.[40] In addition, any catalytic activity observed was unlikely to be influenced the SiO_2, which is generally thought to be nonparticipating.[3] Control experiments, using both bare fumed silica and AuNP assembled on the high surface area support without ozone treatment, were performed by adding 0.1 g of each solid to an IR gas cell that had been flushed with N_2 before the addition of equal molar concentrations of O_2 and CO. Neither of these untreated samples demonstrated measurable catalytic activity. A sample of the AuNPs on the high surface area support was treated with dilute ozone and rinsed as described

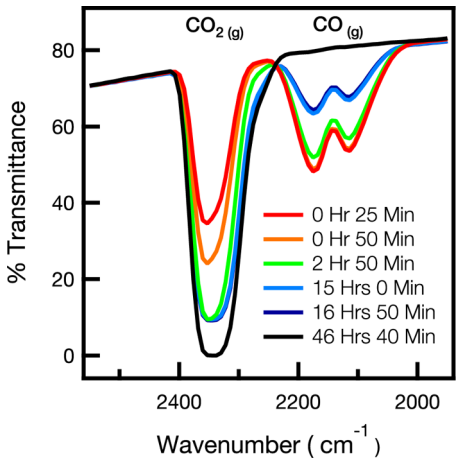

Figure 6. FT-IR spectra for a gas cell containing ozone-treated and rinsed AuNP assemblies on fumed silica and 3 mL each O_2 and CO. Catalytic oxidation of CO is indicated by the decreasing peaks for CO at 2150 cm^{-1} and the growth of peaks for CO_2 at 2450 cm^{-1}. The spectra were normalized at 2600 cm^{-1} to correct for changes in cell position.

previously. Following lyophilization, 0.1 g of the solid was added to the IR gas cell, flushed as before, and charged with CO and O_2. The conversion of the CO to CO_2 was monitored until the reaction had gone to completion (Figure 6).

Given that thiols poison the surfaces of gold catalysts,[11] the catalytic activity observed confirms that ozone treatment and rinsing produces an active gold surface. Additional confirmation that a reactive gold surface has been generated comes from the rapid reaction of those surfaces with added thiol. A sample of the ozone treated and rinsed AuNP assemblies on the planar analysis platform were placed in a 1 mM 2-MEPA ligand solution for 1 and 10 min and characterized using high resolution XPS scans of the S 2p region (Figure S3). An increase in reduced sulfur and loss of the small amount of oxidized sulfur remaining on the surface after ozone treatment occurs within 1 min; no further change occurs during the subsequent 10 min of soaking. In contrast, place exchange reactions of thiol typically reach equilibrium on the order of hours to days.[47] This method may therefore afford a facile method for installation of other ligand functionalities without lengthy treatment times.

To summarize, the combined data from XPS analysis and CO oxidation obtained from oxidized and rinsed assemblies provide a picture of the physical and chemical changes that occur over the course of ligand removal from supported AuNPs. A portion of the ligand shell was oxidized during treatment, and we hypothesized that remaining ligands continue to tether the particles to the surface allowing the oxidized sulfur to be rinsed away with water, affording access to the active gold surface.

Characterizing the Stepwise Removal of Ligands from Supported 1.4 nm 2-MEPA AuNPs. To characterize the extent of

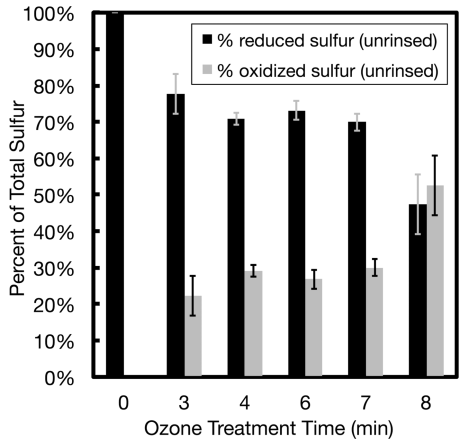

Figure 7. Amounts of reduced sulfur (thiolate) and oxidized sulfur species resulting from exposure in dilute ozone from 0 to 8 min based upon the S 2p peak area ratios. Each treatment time was sampled over three spots to account for surface variation and error bars represent one standard deviation from the mean. Peaks were fit to S 2p trace and each percentage calculated from the sum of oxidized (168 eV) and reduced (162 eV) calculated area.

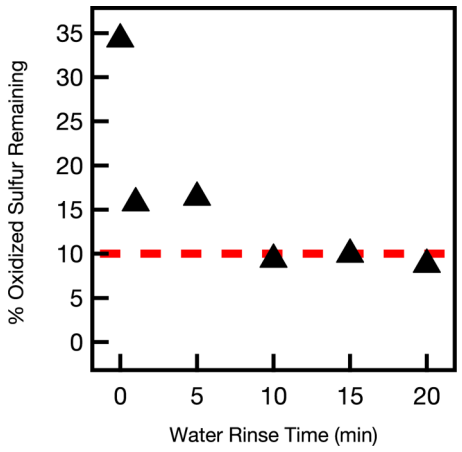

Figure 8. Amount of oxidized ligand remaining on the gold nanoparticle surface *versus* the rinsing time. After 10 min the number of ligands remained stable at 10% as designated by the dashed line. The percentage of ligands was calculated from XPS ratios of oxidized to reduced sulfur 2p peaks as described in Figure 7.

ligand removal as a function of ozone treatment time, we employed TEM and XPS analysis of assemblies of the 1.4 nm 2-MEPA AuNPs on the planar characterization platform. Samples were introduced into the dilute ozone gas stream, and pairs of samples were removed at various time points for analysis. One of each pair was analyzed by XPS and TEM, while the other was first rinsed with nanopure water before the same analysis (Figure S4). The ratio (as a percentage of total sulfur) of oxidized sulfur (B.E. 168 eV) to bound thiolate ligand (B.E. 162 eV) was determined by XPS analysis (Figure 7).

The duration of ozone exposure, as well as the subsequent rinse time, was optimized to expose as much of the active gold surface as possible while maintaining covalent tethering and preserving the average particle size. A dilute ozone treatment time of 8 min was chosen as an ideal treatment point from the observed crossover between oxidized and reduced sulfur at this point contrasted to the roughly 20% oxidized it had attained after only about 3 min of ozone treatment and a relatively steady 30% oxidized over the next 5 min. The removal of the oxidized ligands by rinsing with water was optimized for a set of samples exposed to dilute ozone for 8 min. These samples were then placed in 20 mL of nanopure water and allowed to soak for between 1 to 20 min. The samples were removed one by one, dried under a dilute stream of argon, and then analyzed by XPS. Analysis of these samples showed that the amount of oxidized sulfur remaining leveled off after 10 min in water, so this was taken as the optimal rinse time (Figure 8).

The relative amounts of reduced and oxidized[31,48] sulfur throughout the treatments can be used to determine the number of ligands involved in each process (Table 2). 1.5 nm 2-MEPA functionalized AuNPs have previously been well characterized and shown to have an average of 35 ligands bound to the surface of the gold core.[38] Because the average particle size does not change over the course of treatment (Table 1) the number and type of ligands involved in each treatment step can be calculated. Initially, all 35 ligands are in the form of bound thiolate. Following 8 min of exposure to the 50 ppm ozone gas stream the *average* particle contains 52.6% oxidized sulfur and 47.4% bound thiolate indicating that 17 ligands remain unchanged while 18 of the ligands have been oxidized.[31,48] Although it was not possible to determine the spatial distribution of the remaining ligands by XPS, reports using sum frequency spectroscopy on much larger AuNPs (>15 nm) during the initial stages of ligand oxidation suggest the preferential oxidation of ligands on the top half of gold nanoparticles.[49]

TABLE 2. Number of Ligands Oxidized and Removed during Ozone Treatment

	number of ligands per particle[a]		
treatment step	bound (reduced)	oxidized	removed
initial	35	—	—
ozone treated	17	18	—
ozone treated and rinsed	17	8	10

[a] Calculated on the basis of the ratio of oxidized to reduced sulfur for an *average* 1.5 nm AuNP with 35 2-MEPA ligands.

After 10 min of water rinsing, the ratio of oxidized sulfur to thiolate decreases (33.1% oxidized sulfur and 66.9% bound thiolate) due to release of some of the oxidized sulfur. Because the thiol ligands are stable for days in nanopure water, it is reasonable to assume that the 66.9% thiolate signal comes from the same 17 bound thiolate ligands; that is, no thiolate is rinsed

away. It follows that there were still approximately 8 oxidized sulfur atoms remaining following treatment. We can therefore reason that the mild ozone treatment followed by a room temperature water soak was able to remove 10 of the 35 thiols initially found in the ligand shell of a 1.5 nm 2-MEPA functionalized AuNP, revealing an active gold surface.

CONCLUSION

We examined the reactivity of ozone with surface-confined alkanethiolate-stabilized AuNPs and showed that ligands can be successfully removed from NPs tethered to an oxide support while leaving the particle core attached and unchanged. This approach, using ligand-stabilized nanoparticles for assembly on a support, offers several advantages over other methods previously demonstrated for creating supported gold clusters. Specifically, it is possible to precisely control and thoroughly analyze the size and composition of the nanostructures prior to assembly. It is also possible to direct the assembly of nanoparticles to specific patterned regions on the surface through the terminal functional groups on the ligand shell.[34] In the present example, the terminal phosphonate groups directed assembly onto the SiO_2 supports used.

We also demonstrated the utility of using two complementary analytical platforms to address the challenge of characterizing chemical transformations of NPs and their ligands on surfaces. The removal of ligands with dilute ozone was confirmed by measuring the catalytic activity of the gold surface. The activity of these supported AuNPs suggests efficient ligand removal. Using the planar grid structure, we examined the chemical transformations of the ligand shell that occurred during oxidative ligand removal. XPS analysis confirmed that some thiol remained on the AuNPs and tethered it to the SiO_2 surface even after oxidation and rinse. TEM size analysis showed that particle growth did not occur and ICP-OES confirmed that AuNPs were not lost during treatment.

The assembly of ligand-stabilized NPs on surfaces, followed by oxidation and removal of thiols may constitute a general approach to produce surface-active nanostructures on surfaces given the widespread use of thiol ligands[48,49] and the susceptibility of those ligands to oxidation.[50] By lowering the affinity of the ligands for the nanoparticle surface, ligands can be removed at room temperature without causing core growth or loss of material from the support, thus maintaining and revealing their valuable size-dependent properties. In addition, the use of dilute ozone provides a degree of control over the extent of removal of ligands.

Finally, ligand removal may advance the use of ligand-protected nanoparticles as precursors for thin film formation. In these cases preservation of the core diameter is not a concern; however, removal of the ligand directly by thermal sintering can be problematic because flexible substrates may not tolerate the high temperatures required for ligand removal. However, a ligand removal treatment like the one demonstrated herein, that degrades the ligand shell prior to thermal treatment, can reduce the temperature required for core fusion enough to be compatible with these sensitive substrates.[50,51]

METHODS

Gold Nanoparticle Synthesis. The nanomaterials used for experiments were all 1.4 nm gold nanoparticles (AuNPs). Synthesis of triphenylphosphine-stabilized particles was accomplished through a sodium borohydride reduction of $HAuCl_4$, triphenylphosphine, and TOAB in water and toluene following the literature preparation.[38] Biphasic ligand exchange was performed with (2-mercaptoethyl)phosphonic acid (2-MEPA) ligand synthesized from a literature preparation.[34] Exchanged particles were purified using a diafiltration membrane[39] with 100 volume equivalents of nanopure water. Following purification, 1.4 nm 2-MEPA AuNPs were concentrated, lyophilized, and stored in the freezer until use.[34]

High Surface Area Support Preparation. Two aliquots of 0.5 g of fumed silica were placed in 20 mL centrifuge tubes. A 15 mL solution containing 5 mM $HfOCl_2$ was added to the silica with a stir bar. This solution was stirred for 2 days. Hf(IV)-functionalized silica was pelleted by centrifugation and resuspended in nanopure water. This process was repeated three times to adequately rinse the sample.

Gold Nanoparticle Assembly on Fumed Silica. Into each centrifuge tube of Hf(IV) functionalized silica was added 15 mL of gold soak solution (1.6 mg of 1.4 nm 2-MEPA AuNPs)/(1 mL of 3/1 MeOH/H_2O) and the mixture stirred for 2 days. The 2-MEPA AuNP-decorated fumed silica was pelleted by centrifugation and resuspended in 15 mL of nanopure water. This process was repeated three times to rinse the sample. The rinsed material was lyophilized and stored in the freezer until use.

Planar Analysis Platform Preparation. To prepare the Smart Grid substrate for TEM and XPS analysis, a silicon wafer was diced into chips and an thermal oxide layer grown by heating it at 1100 °C in O_2 for 13 min. Positive photoresist was used to establish window boundaries. The oxide was etched in diluted buffered oxide etch and the silicon was etched away soaking in 10% TMAH solution at 60 °C for 8 h to reveal windows.[33]

Tethering 1.4 nm 2-MEPA Gold Nanoparticles to Analysis Platform. Grids were cleaned with oxygen plasma and soaked for 15 min in a dilute NH_4OH and H_2O_2 solution to maximize the concentration of surface silanol groups. Grids were rinsed in nanopure water prior to soaking overnight in 5 mM Hf(IV). AuNP tethering to the bound Hf(IV) sites was afforded with an overnight soak (1.6 mg-1.4 nm 2-MEPA AuNPs)/(1 mL 3:1 MeOH:H_2O).[34]

***Ex Situ* Ozone Generation and Dilution.** Ozone was produced by pumping dry air into a corona ozone generator. The concentration of the undiluted ozone was determined to be 500 ppm by an Ozone 10/a Draeger tube and UV−vis absorption at 253.7 nm. By diluting the ozone-enriched gas stream with $N_{2(g)}$, the concentration was lowered to approximately 50 ppm (as measured by 10/a Draeger tube and UV−vis absorption at 253.7 nm).

Removal of Ligand from 1.5 nm Gold Nanoparticles Tethered to Fumed Silica. To remove the ligands from AuNPs tethered to fumed silica, 0.9 g of AuNP-functionalized fumed silica was placed in a 50 mL crystallization dish with a stir bar inside a sealed ozone treatment chamber and stirred. Ozone was flowed into the chamber over 20 min. Following ozone treatment, the chamber

was flushed with N_2. Material was removed from chamber and rinsed using nanopure water into a centrifuge tube and rinsed three times with 15 mL of nanopure water with 15 mL nanopure water. Following the final rinse, samples were resuspended in nanopure water, frozen over dry ice, and recovered as a dry powder by lyophilization.

CO Oxidation as a Functional Assay of the Nanoparticle Surface. To evaluate the reactivity of the AuNP surface, 0.1 g of dry activated fumed silica was added to a IR gas cell with CaF_2 windows that had been flushed with N_2, the IR sample chamber was again flushed with N_2 for 20 min, and a background spectrum was taken. Next, 3 mL of O_2 and 3 mL of CO were injected into the IR cell, and spectra were taken to monitor the conversion of CO to CO_2. FT-IR spectra were collected using a Thermo Scientific Nicolet 6700 spectrometer at a resolution of 16 cm^{-1} to improve signal-to-noise.[52]

XPS Chemical Characterization. XPS spectra were taken at 20 eV pass energy with a ThermoFisher ESCALab 250 with a monochromated Al K-alpha, using a 400 μm spot size. The number of scans was determined empirically to obtain optimal signal/noise.

XPS Sulfur 2p Background Subtraction. To quantify the oxidation of sulfur 2p peaks using XPS we adjusted for the presence of the silicon loss feature in our spectral window. Baseline correction was performed by taking spectra from Hf functionalized platform (blank) and subtracting these spectra from samples of interest. Gain correction was required to adjust for differences in peak intensity, but peaks were not shifted on the binding energy scale. Background subtraction was performed in the program *Avantage* for ease of comparison with other peaks (Figure S5). This technique facilitated quantification of a signal masked by the silicon shake up feature present due to our silica platform.

TEM Microscopy and Nanoparticle Size Determination. Bright-field TEM micrographs were taken using an FEI Tecnai Spirit TEM operated at 120 kV or FEI Titan TEM operated at 300 kV. For each sample a size distribution was determined from multiple representative micrographs using image analysis software (ImageJ). High magnification is used to verify the deposition of a single layer of particles as well as particle morphology prior to acquisition at an appropriate magnification to capture 300−500 particles per micrograph. In order to provide a statistically significant population, several thousand particles were analyzed for each sample. The size distribution is generated by number of particles by established protocols for image analysis as described previously.[43] Briefly, a threshold is applied so that the black and white composite images were representative of the original scanned photos when overlaid prior to automated size analysis by a best-fit ellipse.[43]

ICP-OES Determination of Gold Loading and Particle Desorption. *Aqua regia* was made from concentrated, high purity, 3:1 nitric acid:hydrochloric acid. To determine gold loading on the fumed silica, 6 mg samples of AuNP-decorated fumed silica were digested in 0.75 mL of *aqua regia*, diluted to 15 mL with nanopure water and analyzed by ICP-OES. To determine if gold was lost during ozone treatment, following the rinse step, one milliliter of the rinsate was digested in 0.3 mL of *aqua regia*, diluted to 15 mL with nanopure water and analyzed by ICP-OES. ICP-OES data was taken on a Teledyne Leeman Prodigy running with standard operating parameters in axial mode.

Conflict of Interest: The authors declare no competing financial interest.

Acknowledgment. We acknowledge the Air Force Research Laboratory (under agreement FA8650-05-1-5041), the Center for Sustainable Materials (CHE-1102637), and the National Science Foundation Graduate STEM Fellows in K-12 Education Program under Grant No. DGE-0742540 for financial support. The CAMCOR TEM and XPS facility is supported in grants from the W.M. Keck Foundation, the M.J. Murdock Charitable Trust, the Oregon Nanoscience and Microtechnologies Institute and the University of Oregon.

Supporting Information Available: Representative TEM micrographs of AuNPs during ozone treatment, additional XPS data with oxidized to reduced sulfur ratios throughout ligand removal and ligand shell restoration, and data demonstrating background removal from the S2p region. This material is available free of charge *via* the Internet at http://pubs.acs.org.

REFERENCES AND NOTES

1. Saha, K.; Agasti, S. S.; Kim, C.; Li, X.; Rotello, V. M. Gold Nanoparticles in Chemical and Biological Sensing. *Chem. Rev.* **2012**, *112*, 2739–2779.
2. Della Pina, C.; Falletta, E.; Prati, L.; Rossi, M. Selective Oxidation Using Gold. *Chem. Soc. Rev.* **2008**, *37*, 2077–2095.
3. Haruta, M. Nanoparticulate Gold Catalysts for Low-Temperature CO Oxidation. *J. New Mater. Electrochem. Syst.* **2004**, *7*, 163–172.
4. Lan, X.; Masala, S.; Sargent, E. H. Charge-Extraction Strategies for Colloidal Quantum Dot Photovoltaics. *Nat. Mater.* **2014**, *13*, 233–240.
5. Linic, S.; Christopher, P.; Ingram, D. B. Plasmonic-Metal Nanostructures for Efficient Conversion of Solar to Chemical Energy. *Nat. Mater.* **2011**, *10*, 911–921.
6. Wang, J.; Lee, Y.-J.; Chadha, A. S.; Yi, J.; Jespersen, M. L.; Kelley, J. J.; Nguyen, H. M.; Nimmo, M.; Malko, A. V.; Vaia, R. A.; *et al.* Effect of Plasmonic Au Nanoparticles on Inverted Organic Solar Cell Performance. *J. Phys. Chem. C* **2012**, *117*, 85–91.
7. Brust, M.; Walker, M.; Bethell, D.; Schiffrin, D. J.; Whyman, R. Synthesis of Thiol-Derivatised Gold Nanoparticles in a Two-Phase Liquid−Liquid System. *J. Chem. Soc., Chem. Commun.* **1994**, 801–802.
8. Ojea-Jiménez, I.; Bastús, N. G.; Puntes, V. Influence of the Sequence of the Reagents Addition in the Citrate-Mediated Synthesis of Gold Nanoparticles. *J. Phys. Chem. C* **2011**, *115*, 15752–15757.
9. Lohse, S. E.; Dahl, J. A.; Hutchison, J. E. Direct Synthesis of Large Water-Soluble Functionalized Gold Nanoparticles Using Bunte Salts as Ligand Precursors. *Langmuir* **2010**, *26*, 7504–7511.
10. Oh, E.; Susumu, K.; Goswami, R.; Mattoussi, H. One-Phase Synthesis of Water-Soluble Gold Nanoparticles with Control over Size and Surface Functionalities. *Langmuir* **2010**, *26*, 7604–7613.
11. Bond, G.; Louis, C.; Thompson, D. T. *Catalysis by Gold*; Imperial College Press: London, 2006; Vol. 6.
12. Lopez-Sanchez, J. A.; Dimitratos, N.; Hammond, C.; Brett, G. L.; Kesavan, L.; White, S.; Miedziak, P.; Tiruvalam, R.; Jenkins, R. L.; Carley, A. F.; *et al.* Facile Removal of Stabilizer-Ligands from Supported Gold Nanoparticles. *Nat. Chem.* **2011**, *3*, 551–556.
13. Jespersen, M. L.; Inman, C. E.; Kearns, G. J.; Foster, E. W.; Hutchison, J. E. Alkanephosphonates on Hafnium-Modified Gold: A New Class of Self-Assembled Organic Monolayers. *J. Am. Chem. Soc.* **2007**, *129*, 2803–2807.
14. Pursell, C. J.; Chandler, B. D.; Manzoli, M.; Boccuzzi, F. CO Adsorption on Supported Gold Nanoparticle Catalysts: Application of the Temkin Model. *J. Phys. Chem. C* **2012**, *116*, 11117–11125.
15. Kilmartin, J.; Sarip, R.; Grau-Crespo, R.; Di Tommaso, D.; Hogarth, G.; Prestipino, C.; Sankar, G. Following the Creation of Active Gold Nanocatalysts from Phosphine-Stabilized Molecular Clusters. *ACS Catal.* **2012**, *2*, 957–963.
16. Menard, L. D.; Xu, F.; Nuzzo, R. G.; Yang, J. C. Preparation of TiO_2-Supported Au Nanoparticle Catalysts from a Au_{13} Cluster Precursor: Ligand Removal Using Ozone Exposure *Versus* a Rapid Thermal Treatment. *J. Catal.* **2006**, *243*, 64–73.
17. Ansar, S. M.; Ameer, F. S.; Hu, W.; Zou, S.; Pittman, C. U.; Zhang, D. Removal of Molecular Adsorbates on Gold Nanoparticles Using Sodium Borohydride in Water. *Nano Lett.* **2013**, *13*, 1226–1229.
18. Tsubota, S.; Nakamura, T.; Tanaka, K.; Haruta, M. Effect of Calcination Temperature on the Catalytic Activity of Au Colloids Mechanically Mixed with TiO_2 Powder for CO Oxidation. *Catal. Lett.* **1998**, *56*, 131–135.

19. Comotti, M.; Li, W.-C.; Spliethoff, B.; Schüth, F. Support Effect in High Activity Gold Catalysts for CO Oxidation. *J. Am. Chem. Soc.* **2005**, *128*, 917–924.
20. Sze, C.; Gulari, E.; Demczyk, B. G. Structure of Coprecipitated Gold−Iron Oxide Catalyst Materials. *Mater. Lett.* **1998**, *36*, 11–16.
21. Ma, Z.; Dai, S. Design of Novel Structured Gold Nanocatalysts. *ACS Catal.* **2011**, *1*, 805–818.
22. Yan, W.; Mahurin, S. M.; Pan, Z.; Overbury, S. H.; Dai, S. Ultrastable Au Nanocatalyst Supported on Surface-Modified TiO_2 Nanocrystals. *J. Am. Chem. Soc.* **2005**, *127*, 10480–10481.
23. Zanella, R.; Giorgio, S.; Henry, C. R.; Louis, C. Alternative Methods for the Preparation of Gold Nanoparticles Supported on TiO_2. *J. Phys. Chem. B* **2002**, *106*, 7634–7642.
24. Yang, Y.-F.; Sangeetha, P.; Chen, Y.-W. Au/FeOx−TiO_2 Catalysts for the Preferential Oxidation of CO in a H_2 Stream. *Ind. Eng. Chem. Res.* **2009**, *48*, 10402–10407.
25. Smith, B. L.; Hutchison, J. E. Transformations During Sintering of Small (D_{core} < 2 nm) Ligand-Stabilized Gold Nanoparticles: Influence of Ligand Functionality and Core Size. *J. Phys. Chem. C* **2013**, *117*, 25127–25137.
26. Sperling, R. A.; Parak, W. J. Surface Modification, Functionalization and Bioconjugation of Colloidal Inorganic Nanoparticles. *Philos. Trans. R. Soc., A* **2010**, *368*, 1333–1383.
27. Tomczak, N.; Jańczewski, D.; Tagit, O.; Han, M.-Y.; Vancso, G. J. Surface Engineering of Quantum Dots with Designer Ligands. In *Surface Design: Applications in Bioscience and Nanotechnology*; Wiley-VCH Verlag GmbH & Co. KGaA: Weinheim, 2009; pp 341−361.
28. Worley, C. G.; Linton, R. W. Removing Sulfur from Gold Using Ultraviolet/Ozone Cleaning. *J. Vac. Sci. Technol., A* **1995**, *13*, 2281–2284.
29. King, D. E. Oxidation of Gold by Ultraviolet Light and Ozone at 25 °C. *J. Vac. Sci. Technol., A* **1995**, *13*, 1247–1253.
30. Zhang, Y.; Terrill, R. H.; Bohn, P. W. Ultraviolet Photochemistry and *Ex Situ* Ozonolysis of Alkanethiol Self-Assembled Monolayers on Gold. *Chem. Mater.* **1999**, *11*, 2191–2198.
31. Norrod, K. L.; Rowlen, K. L. Ozone-Induced Oxidation of Self-Assembled Decanethiol: Contributing Mechanism for "Photooxidation"? *J. Am. Chem. Soc.* **1998**, *120*, 2656–2657.
32. Hajati, S.; Tougaard, S. XPS for Non-Destructive Depth Profiling and 3D Imaging of Surface Nanostructures. *Anal. Bioanal. Chem.* **2010**, *396*, 2741–2755.
33. Kearns, G. J.; Foster, E. W.; Hutchison, J. E. Substrates for Direct Imaging of Chemically Functionalized SiO_2 Surfaces by Transmission Electron Microscopy. *Anal. Chem.* **2006**, *78*, 298–303.
34. Foster, E. W.; Kearns, G. J.; Goto, S.; Hutchison, J. E. Patterned Gold-Nanoparticle Monolayers Assembled on the Oxide of Silicon. *Adv. Mater.* **2005**, *17*, 1542–1545.
35. Campbell, C. T. The Active Site in Nanoparticle Gold Catalysis. *Science* **2004**, *306*, 234–235.
36. Neff, G. A.; Page, C. J.; Meintjes, E.; Tsuda, T.; Pilgrim, W. C.; Roberts, N.; Warren, W. W. Hydrolysis of Surface-Bound Phosphonate Esters for the Self-Assembly of Multilayer Films: Use of Solid State Magic Angle Spinning ^{31}P NMR as a Probe of Reactions on Surfaces. *Langmuir* **1996**, *12*, 238–242.
37. Hong, H. G.; Sackett, D. D.; Mallouk, T. E. Adsorption of Well-Ordered Zirconium Phosphonate Multilayer Films on High Surface Area Silica. *Chem. Mater.* **1991**, *3*, 521–527.
38. Woehrle, G. H.; Brown, L. O.; Hutchison, J. E. Thiol-Functionalized, 1.5-nm Gold Nanoparticles through Ligand Exchange Reactions: Scope and Mechanism of Ligand Exchange. *J. Am. Chem. Soc.* **2005**, *127*, 2172–2183.
39. Sweeney, S. F.; Woehrle, G. H.; Hutchison, J. E. Rapid Purification and Size Separation of Gold Nanoparticles *via* Diafiltration. *J. Am. Chem. Soc.* **2006**, *128*, 3190–3197.
40. Haruta, M. Gold as a Novel Catalyst in the 21st Century: Preparation, Working Mechanism and Applications. *Gold Bull.* **2004**, *37*, 27–36.
41. Dasog, M.; Scott, R. W. J. Understanding the Oxidative Stability of Gold Monolayer-Protected Clusters in the Presence of Halide Ions under Ambient Conditions. *Langmuir* **2007**, *23*, 3381–3387.
42. Dugas, V.; Chevalier, Y. Surface Hydroxylation and Silane Grafting on Fumed and Thermal Silica. *J. Colloid Interface Sci.* **2003**, *264*, 354–361.
43. Woehrle, G. H.; Hutchison, J. E.; Ozkar, S.; Finke, R. G. Analysis of Nanoparticle Transmission Electron Microscopy Data Using a Public- and Domain Image-Processing Program, Image. *Turk. J. Chem.* **2006**, *30*, 1–13.
44. Bourg, M.-C.; Badia, A.; Lennox, R. B. Gold−Sulfur Bonding in 2D and 3D Self-Assembled Monolayers: XPS Characterization. *J. Phys. Chem. B* **2000**, *104*, 6562–6567.
45. Lindberg, B. J.; Hamrin, K.; Johansson, G.; Gelius, U.; Fahlman, A.; Nordling, C.; Siegbahn, K. Molecular Spectroscopy by Means of ESCA II. Sulfur Compounds. Correlation of Electron Binding Energy with Structure. *Phys. Scr.* **1970**, *1*, 286.
46. Castner, D. G.; Hinds, K.; Grainger, D. W. X-Ray Photoelectron Spectroscopy Sulfur 2p Study of Organic Thiol and Disulfide Binding Interactions with Gold Surfaces. *Langmuir* **1996**, *12*, 5083–5086.
47. Hostetler, M. J.; Templeton, A. C.; Murray, R. W. Dynamics of Place-Exchange Reactions on Monolayer-Protected Gold Cluster Molecules. *Langmuir* **1999**, *15*, 3782–3789.
48. Johnson, B. N.; Mutharasan, R. Regeneration of Gold Surfaces Covered by Adsorbed Thiols and Proteins Using Liquid-Phase Hydrogen Peroxide-Mediated UV-Photooxidation. *J. Phys. Chem. C* **2012**, *117*, 1335–1341.
49. Pang, S.; Kurosawa, Y.; Kondo, T.; Kawai, T. Decomposition of Monolayer Coverage on Gold Nanoparticles by UV/Ozone Treatment. *Chem. Lett.* **2005**, *34*, 544–545.
50. Weber, D.; Sharma, R.; Botnaras, S.; Pham, D. V.; Steiger, J.; De Cola, L. Base-Etch Removal of a Ligand Shell in Thin Films of ZnO Nanoparticles for Electronic Applications. *J. Mater. Chem. C* **2013**, *1*, 7111–7116.
51. Weber, D.; Botnaras, S.; Pham, D. V.; Steiger, J.; De Cola, L. Functionalized ZnO Nanoparticles for Thin-Film Transistors: Support of Ligand Removal by Non-Thermal Methods. *J. Mater. Chem. C* **2013**, *1*, 3098–3103.
52. Bak, J.; Clausen, S. Signal-to-Noise Ratio of FT-IR CO Gas Spectra. *Appl. Spectrosc.* **1999**, *53*, 697–700.